https://doi.org/10.5194/cp-2023-81
Preprint. Discussion started: 4 October 2023
© Author(s) 2023. CC BY 4.0 License.

Climate of the Past Discussions

New estimation of critical insolation – CO_2 relationship for triggering glacial inception

Stefanie Talento[1], Matteo Willeit[1] and Andrey Ganopolski[1]

[1]Potsdam Institute for Climate Impact Research, Potsdam, 14473, Germany

Correspondence to: Stefanie Talento (talento@pik-potsdam.de)

Abstract.

It has been previously proposed that glacial inception represents a bifurcation transition between interglacial and glacial states, and is governed by the non-linear dynamics of the climate-cryosphere system. To trigger glacial inception, the orbital forcing (defined as the maximum of summer insolation at 65ºN and determined by Earth's orbital parameters) must be lower than a critical level, which depends on the atmospheric CO_2 concentration. While paleoclimatic data do not provide a strong constraint on the dependence between CO_2 and critical insolation, its accurate estimation is of fundamental importance for predicting future glaciations and the effect that anthropogenic CO_2 emissions might have on them.

In this study, we use the novel Earth system model of intermediate complexity CLIMBER-X with interactive ice sheets to produce a new estimation of the critical insolation - CO_2 relationship for triggering glacial inception. We perform a series of experiments in which different combinations of orbital forcing and atmospheric CO_2 concentration are maintained constant in time. We analyse for which combinations of orbital forcing and CO_2 glacial inception occurs and trace the critical relationship between them, separating conditions under which glacial inception is possible from those where glacial inception is not materialised. We also provide a theoretical foundation for the proposed critical insolation – CO_2 relation.

We find that the use of the maximum summer insolation at 65°N as a single metric for orbital forcing is adequate for tracing the glacial inception bifurcation. Moreover, we find that the temporal and spatial patterns of ice sheet growth during glacial inception are not always the same but depend on the critical insolation and CO_2 level. The experiments evidence that during glacial inception, ice sheets grow mostly in North America, and only under low CO_2 conditions ice sheets are also formed over Scandinavia. The latter is associated with a weak Atlantic Meridional Overturning Circulation (AMOC) for low CO_2. We find that the strength of AMOC also affects the rate of ice sheet growth during glacial inception.

https://doi.org/10.5194/cp-2023-81
Preprint. Discussion started: 4 October 2023
© Author(s) 2023. CC BY 4.0 License.

Climate of the Past Discussions

1 Introduction

Glacial cycles are the dominant mode of climatic variability over the last 2.7 million years. The timing of glaciations and deglaciations is primarily controlled by changes in Earth's orbital parameters through the modulation of the amount of solar radiation received in high latitudes of the Northern Hemisphere (NH) during boreal summer (Milankovitch, 1941).

Using an Earth system model of intermediate complexity (EMIC), Calov et al. (2005) proposed that glacial inception represents a bifurcation transition from interglacial to glacial states of the Earth system. When summer insolation at high latitudes of the NH falls below a certain threshold, the interglacial state becomes unstable and ice sheet growth begins. The process is amplified through non-linear feedbacks, of which the snow and ice-albedo and the elevation feedbacks are the dominant ones. Eventually, large ice sheets develop over the North American and the Eurasian continents.

The threshold value for boreal summer insolation to trigger a glacial inception depends on the atmospheric concentration of greenhouse gases, among which CO_2 is, by far, the most important (Köhler et al., 2010). While paleoclimatic data do not constrain this dependence, its accurate estimation is of fundamental importance for predicting future glaciations and the effect that anthropogenic CO_2 emissions might have on them (Archer and Ganopolski, 2005; Talento and Ganopolski, 2021).

The first attempt at tracing the relationship between insolation and CO_2 for triggering glacial inception was performed in Archer and Ganopolski (2005) using the EMIC CLIMBER-2 (Petoukhov et al., 2000, Ganopolski et al. 2001). This first estimation was, however, rather crude as it was based only on a small set of relatively short experiments that did not allow for the detection of the bifurcation with sufficient accuracy. Ganopolski et al. (2016) updated the results also using CLIMBER-2 with a new methodology that allowed for increased accuracy. The authors proposed a functional relationship between summer maximum insolation at 65° N (smx65) and CO_2 for triggering glacial inception. The relationship describes the critical smx65 for the onset of glaciation as linearly dependent on the logarithm of CO_2: $smx65_{cr} = \alpha \ln(CO_2/CO_{2\_0}) + \beta$, where CO_2 is the atmospheric CO_2 concentration, CO_{2_0} is a reference atmospheric CO_2 value (for example, the preindustrial value) and α and β are empirical constants.

The shape of the dependency is in agreement with the facts that (i) the radiative forcing of CO_2 follows a logarithmic structure and (ii) that in CLIMBER-2 the temperature response to radiative forcing of CO_2 and orbital forcing is linear within the considered range.

The purpose of this work is to build upon the findings of Ganopolski et al. (2016) and generate a new estimation of the relationship between insolation and atmospheric CO_2 critical for triggering glacial inception, using the recently developed and more advanced CLIMBER-X model (Willeit et al., 2022, 2023a, 2023b). While CLIMBER-X is also an EMIC that shares with

https://doi.org/10.5194/cp-2023-81
Preprint. Discussion started: 4 October 2023
© Author(s) 2023. CC BY 4.0 License.

Climate of the Past Discussions

CLIMBER-2 the principles of computational efficiency and usage of a statistical-dynamical atmospheric model, it represents a significant development compared to the CLIMBER-2 model used in the previous studies (Ganopolski and Brovkin, 2017; Willeit et al., 2019). In particular CLIMBER-X has (i) a much higher horizontal resolution in the atmosphere and land models (5°x5° versus ~50° x 10° in a longitude-latitude grid), (ii) a 3D ocean model, (iii) more internally consistent components and (iv) better treatment of individual processes. Furthermore, we investigate the temporal and spatial patterns of ice sheet growth during glacial inception and the effects of changes in the Atlantic Meridional Overturning Circulation (AMOC) strength on the rate of ice sheets growth. We also analyse the suitability of using the smx65 as a single metric for orbital forcing. A theoretical derivation of the critical insolation – CO_2 relationship for triggering glacial inception is provided in Annex A.

2 Model and experimental setup

2.1 Model description

We employ the new CLIMBER-X EMIC (Willeit et al., 2022, 2023a, 2023b). The model was specifically designed to simulate the Earth system evolution on timescales from decades to hundreds of thousands of years. The climate component of CLIMBER-X consists of: the 2.5-dimensional Semi-Empirical dynamical-Statistical Atmosphere Model (SESAM), the 3-dimensional frictional-geostrophic ocean model GOLDSTEIN, the dynamic-thermodynamic SImple Sea Ice Model (SISIM) and the land surface–vegetation model PALADYN. All the models from the climate core are discretized on a longitude-latitude grid with 5°x5° horizontal resolution and use a daily time-step. CLIMBER-X incorporates the 3-dimensional thermomechanical ice sheet model SICOPOLIS (Greve et al., 2017) via the high-resolution physically-based surface energy and mass balance interface SEMIX and a basal ice shelf melt module. In this study, SICOPOLIS is applied only to the NH with a 32 km horizontal resolution. The viscoelastic solid Earth model VILMA (Klemann et al., 2008; Martinec et al., 2018) is used to simulate the bedrock response to changes in loading by solving the sea-level equation. A detailed description of the coupling between climate and ice sheet components is provided in Willeit et al. (2023b).

Even though CLIMBER-X has a relatively coarse spatial resolution and a simplified treatment of some processes, the number of physical processes included in the model, as well as its performance for the present-day climate, are comparable with state-of-the-art (CMIP6-type) climate models. CLIMBER-X is reasonably successful in reproducing the present-day climatology of variables relevant for the formation of ice sheets. However, near-surface summer temperatures (a key variable for determining ablation of ice sheets) are up to 5°C too warm over the eastern portion of North America when compared to observations. Preliminary experiments show that such biases preclude the realistic development of North American ice-sheets. Therefore, similarly to Ganopolski et al. (2010), we implement a 2m-temperature bias correction in the surface mass balance calculation (see Willeit et al., 2023b). In addition, a uniform offset of -0.5°C is applied globally in the surface mass balance scheme.

https://doi.org/10.5194/cp-2023-81
Preprint. Discussion started: 4 October 2023
© Author(s) 2023. CC BY 4.0 License.


2.2 Experimental setup

We perform a series of equilibrium experiments in which different orbital parameters (obliquity, eccentricity and precession), atmospheric CO_2 concentration, are maintained constant for the whole duration of the simulation. All NH ice sheets are fully interactive and influence climate through albedo, elevation, sea level (which affects land-sea mask) and freshwater flux into the ocean. The Antarctic Ice sheet is not interactive, but fixed at its present-day state. The experiments are performed using an acceleration technique with asynchronous coupling between the climate and ice sheet model components. An acceleration factor of 10 is used, i.e. the climate model component is updated every 10 years of the ice sheet model. Each model simulation is run for 100.000 years of the ice sheet model (corresponding to 10.000 years of the climate model) starting from pre-industrial equilibrium conditions with observed present-day Greenland ice sheet with a uniform ice temperature of -10°C.

We select 19 combinations of orbital parameters corresponding to the 19 local minima of the smx65 time-series of the last 400 kyr, corresponding to values in the range between 430 and 496 W/m^2 (Fig. 1). Therefore, selected combinations of orbital parameters have similar precession but very different eccentricity and obliquity values. For each of these 19 sets of orbital parameters, we produce a series of equilibrium experiments designed to detect the critical insolation – CO_2 relationship for triggering inception. The procedure is, for each set of orbital parameters, as follows:

1. We start from a simulation using a (fairly high) atmospheric CO_2 concentration of 500 ppm, for which glacial inception is not expected to occur under any orbital configuration.

2. If the NH ice volume (v) is < X msle (meters in sea level equivalent) during the whole simulation, we reduce CO_2 by 5 ppm and repeat the simulation.

   If, on the contrary, v is >= X msle at any moment in the simulation, we stop the iteration and define the insolation – CO_2 combination used in this case as critical for glacial inception.

In this study, we select a value of X = 15 msle. That value corresponds to an ice volume roughly twice the value of the present-day Greenland ice sheet volume. As in CLIMBER-X ice volume over Greenland does not increase substantially under glacial inception conditions, 15 msle is thus associated with a considerable ice sheet growth outside Greenland.

To validate the model suitability for tracing glacial inception bifurcation transitions, similarly to Ganopolski et al. (2016), we test the model performance against two paleoclimatic constraints. The first constraint is that, for present-day orbital configuration and atmospheric CO_2 concentration of 280 ppm (named Control simulation, Table 1), the model should not produce any substantial ice growth outside of Greenland. The second constraint is that, on the contrary, for the same 280 ppm level of atmospheric CO_2 concentration but an orbital configuration corresponding to the end of MIS11 (398 kyr BP) a

https://doi.org/10.5194/cp-2023-81
Preprint. Discussion started: 4 October 2023
© Author(s) 2023. CC BY 4.0 License.

Climate of the Past Discussions
Open Access
EGU

significant ice growth, indicative of glacial inception, should occur. Under the current model version these two constraints are met: after 100 kyr of simulation the NH ice volume totals, including the Greenland ice sheet, 8.3 msle for the present-day case and 21 msle for the MIS11 configuration.

Additional experiments with prescribed present-day ice sheets or applying a freshwater hosing/extraction in the North Atlantic Ocean to alter AMOC strength are also conducted for selected orbital forcing-CO_2 configurations (Table 1).

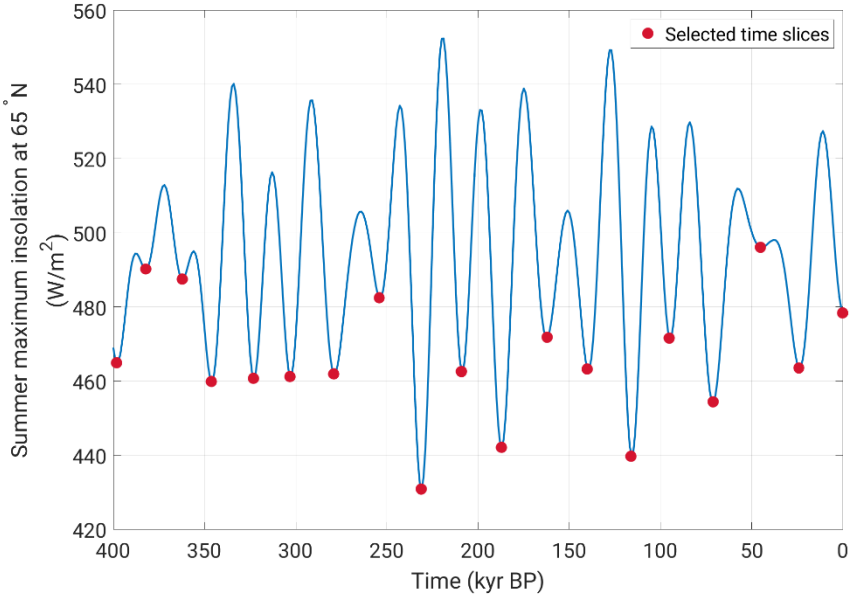

Figure 1: Summer maximum insolation at 65°N (smx65) in the period 400 kyr BP – present, computed using Laskar et al. (2004) data for Earth orbital parameters. Marked in red are all the 19 local minima of the time-series, whose orbital configurations are selected for the CLIMBER-X experiments.

3 Results

3.1 Critical smx65- CO_2 relationship for triggering glacial inception

The usage of smx65 as a proxy for orbital forcing is common practise and considered a good metric for the analysis of glacial inception processes (Ganopolski et al., 2016; Paillard, 1998; Leloup and Paillard, 2022), as the 65°N latitude coincides with the presence of land potentially capable of supporting the initial growth of ice sheets.

https://doi.org/10.5194/cp-2023-81
Preprint. Discussion started: 4 October 2023
© Author(s) 2023. CC BY 4.0 License.

Climate of the Past Discussions

Considering smx65 as orbital forcing indicator, Fig. 2 shows the critical smx65-CO_2 combinations for triggering glacial inception in the 19 individual sets of experiments. Accounting for the fact that the radiative effect of CO_2 is logarithmic and that the temperature response to insolation is linear, we fit the data (via least-squares) with curves of the shape:

$$smx65_{cr} = \alpha \ln(CO_2/280) + \beta \quad (1)$$

The least-squares-fit of the data points produces values of α = -75 W/m^2 and β = 465 W/m^2. The fit is good, with a coefficient of determination R^2 = 0.95. The largest error in the fit is produced for an intermediate insolation case (462 W/m^2, corresponding to the minimum in summer solstice insolation at 209 ka), in which the difference between the least-squares fit and the CLIMBER-X result for the critical CO_2 is ~30 ppm. The new CLIMBER-X estimation for α and β is similar to the one generated with the CLIMBER-2 model and presented in Ganopolski et al. (2016). For that study the criterion for defining glacial inception was comparable (a growth of the NH ice sheets of more than 13.5 msle was required), and the values for α and β were -77 and 466 W/m^2, respectively. The results hint, then, that values for α and β might not be strongly model-dependent. In Annex A we present indeed a conceptual derivation for the values of α and β, confirming the values obtained through the model experiments.

In order to better understand glacial inception at the critical insolation-CO_2 threshold, and to evaluate similarities and differences for diverse insolation/CO_2 pairings, we select three experiments and analyse the temporal and spatial evolution of ice sheet growth. The three experiments (Hsmx65_LCO$_2$, Lsmx65_HCO$_2$ and Ismx65_ICO$_2$) correspond to either the highest, lowest or an intermediate value of the smx65 time-series 19 local minima, respectively. In each experiment, the atmospheric CO_2 corresponds to the critical CO_2 for triggering glacial inception (Table 1). While, by definition, all three experiments Hsmx65_LCO$_2$, Lsmx65_HCO$_2$ and Ismx65_ICO$_2$ reach at least 15 msle NH ice volume at some point during the simulation, they do it with different temporal and spatial dynamics (Fig. 3 and Fig. 4).

https://doi.org/10.5194/cp-2023-81
Preprint. Discussion started: 4 October 2023
© Author(s) 2023. CC BY 4.0 License.

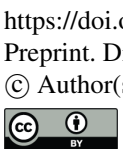

Climate of the Past Discussions
Open Access
EGU

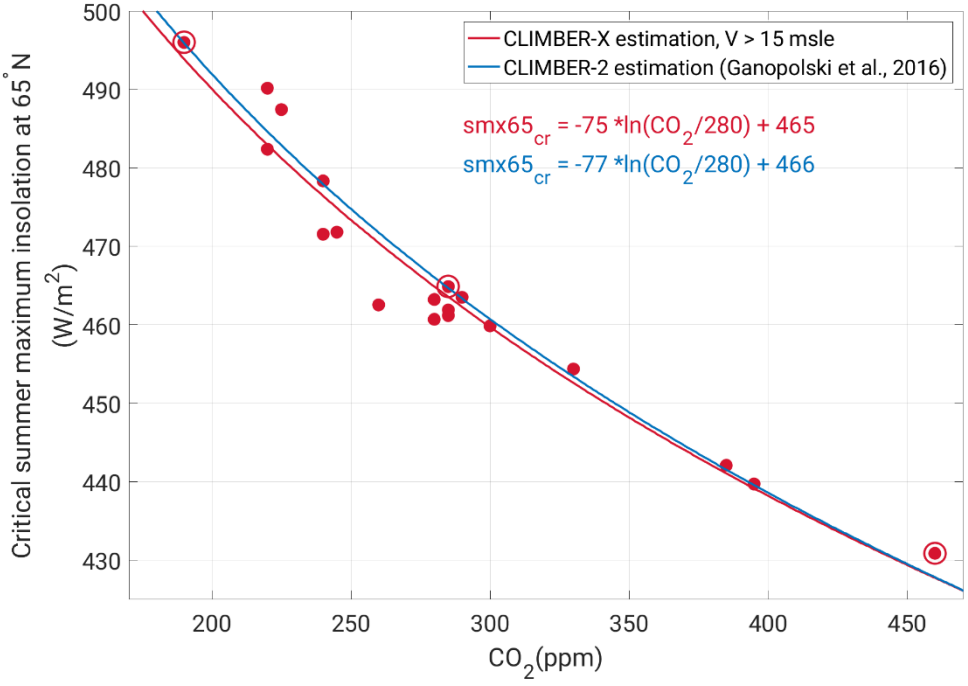

Figure 2: CLIMEBR-X estimation of critical summer maximum insolation at 65°N (smx65) and CO_2 for triggering glacial inception at the threshold of 15 msle (red dots). The red line corresponds to the least-square fit following a logarithmic shape. The CLIMBER-2 estimation from Ganopolski et al. (2016) is depicted in blue. Big red circles indicate the experiments Hsmx65_LCO2, Ismx65_ICO2 and Lsmx65_HCO2.

For the experiment Hsmx65_LCO$_2$ (smx65 = 496 W/m^2 and CO_2 = 190ppm) the NH ice volume time-series crosses the 15 msle threshold 67 kyrs into the simulation and reaches a quasi-equilibrium value of 16.6 msle only after 90 kyrs (Fig. 3). At the moment of crossing the glacial inception threshold (15 msle), the ice-sheets have significantly developed outside of Greenland over Iceland, Svalbard, Novaya Zemlya, and the Scandinavian Peninsula and, in North America, north of Hudson Bay, from 90°W to 70°W (Fig. 4a). The Scandinavian ice sheet development is aided by a weak AMOC (Fig. 5) and subsequent weakened meridional heat transport from the tropics towards that region. The AMOC reaches quasi-equilibrium conditions in the second half of the simulation, with a maximum magnitude of ~16 Sv. At the threshold crossing time, the AMOC is weak and shallow (Fig. 6a) and deep convection in the North Atlantic Ocean only occurs in the Norwegian Sea (Fig. 6d).

https://doi.org/10.5194/cp-2023-81
Preprint. Discussion started: 4 October 2023
© Author(s) 2023. CC BY 4.0 License.

Climate of the Past Discussions

Table 1: Summary of selected experiments' configurations

Experiment name	smx65 (W/m^2)	CO_2 (ppm)	Ice sheets	Freshwater hosing/extraction into North Atlantic
Control	478.3	280	Interactive	-
Control_FixIce	478.3	280	Fixed to present-day	-
Hsmx65_LCO₂	496.0	190	Interactive	-
Hsmx65_LCO₂_FixIce	496.0	190	Fixed to present-day	-
Hsmx65_LCO₂+0.01Sv	496.0	190	Interactive	0.01 Sv
Hsmx65_LCO₂-0.01Sv	496.0	190	Interactive	-0.01 Sv
Ismx65_ICO₂	464.8	285	Interactive	-
Ismx65_ICO₂_FixIce	464.8	285	Fixed to present-day	-
Ismx65_ICO₂+0.01Sv	464.8	285	Interactive	0.01 Sv
Ismx65_ICO₂-0.01Sv	464.8	285	Interactive	-0.01 Sv
Lsmx65_HCO₂	430.8	460	Interactive	-
Lsmx65_HCO₂_FixIce	430.8	460	Fixed to present-day	-
Lsmx65_HCO₂+0.01Sv	430.8	460	Interactive	0.01 Sv
Lsmx65_HCO₂-0.01Sv	430.8	460	Interactive	-0.01 Sv

190

https://doi.org/10.5194/cp-2023-81
Preprint. Discussion started: 4 October 2023
© Author(s) 2023. CC BY 4.0 License.

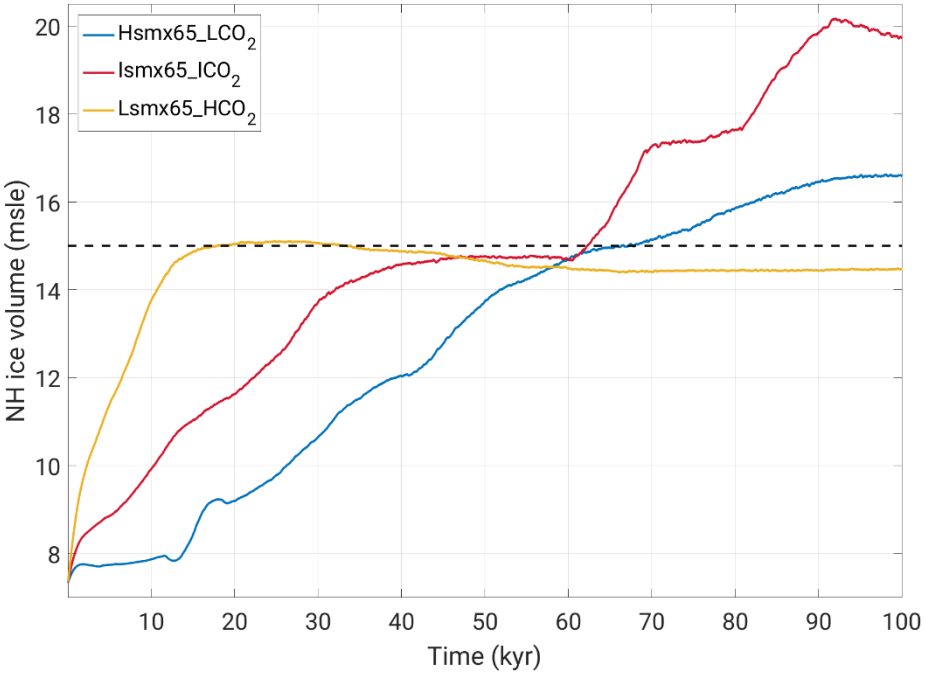

Figure 3: NH ice volume (msle) temporal evolution at the critical combination of smx65 and CO_2 for triggering glacial inception (threshold 15 msle level, dashed line), for three selected experiments (see Table 1).

In the experiment Ismx65_ICO_2 (smx65 = 464.8W/m^2 and CO_2 = 285ppm) the NH ice volume time-series shows a faster increasing rate at the start of the experiment than the Hsmx65_LCO_2 experiment, but stagnates at 14.5 msle between 40 and 60 kyrs of simulation. At 60 kyrs of simulation, the time-series shows an abrupt increase, crossing the 15 msle threshold at time 63 kyr. After that, the time-series stagnates again at ~17.5 msle before showing another abrupt increase towards the end of the simulated period. In the 100 kyrs of simulation, quasi-stationary conditions are not reached (Fig. 3). In this experiment, the AMOC is unstable and oscillates between ~25 Sv and ~16 Sv (Fig. 5). It should be noted that the timescale of these simulated oscillations is distorted by the climate acceleration factor. The AMOC weakening episodes precede the abrupt NH ice volume growths and are, thus, likely triggers. At the moment when the NH ice volume is 15 msle, the ice-sheets cover north of Hudson Bay from 100°W to 70°W (covering almost the totality of Baffin Island), full ice coverage of Iceland, Svalbard and Novaya Zemlya, and partial ice coverage of Scandinavia (Fig. 4c). The moderate ice growth over Scandinavia is related to the AMOC weakening episodes (Fig. 5) and the consequential decreased heat transport from the tropics, as such ice growths is inhibited in simulations with stable AMOC (see Section 3.2 with extraction simulation Ismx65_ICO_2-0.01Sv). At the time of the 15 msle crossing, the Atlantic overturning circulation penetrates until ~3000 m of depth and deep water formation does not occur in the Labrador Sea and south of Greenland (Figs. 6b and 6e).

https://doi.org/10.5194/cp-2023-81
Preprint. Discussion started: 4 October 2023
© Author(s) 2023. CC BY 4.0 License.

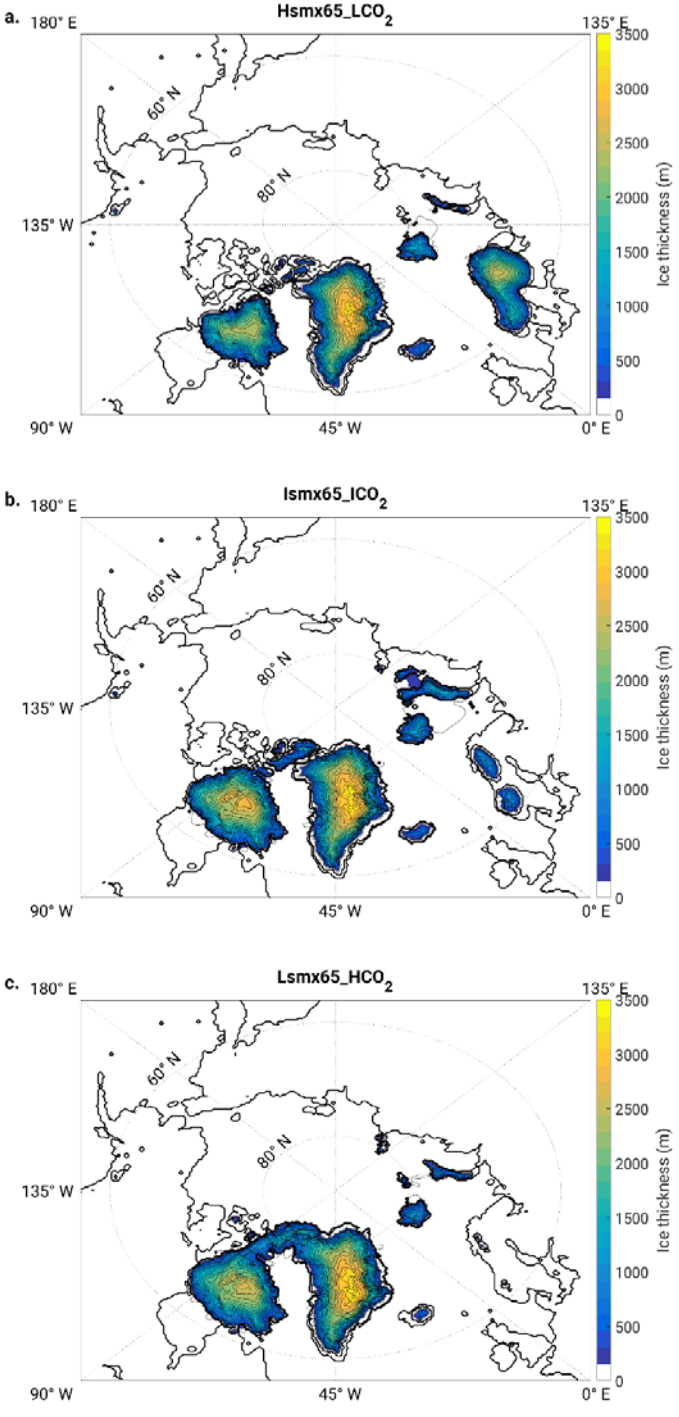

Figure 4: Ice thickness (a-c) for the Hsmx65_LCO$_2$, Ismx65_ICO$_2$ and Lsmx65_HCO$_2$ at the time when each experiment reaches the 15 msle threshold.

https://doi.org/10.5194/cp-2023-81
Preprint. Discussion started: 4 October 2023
© Author(s) 2023. CC BY 4.0 License.

Climate of the Past Discussions
Open Access
EGU

The Lsmx65_HCO_2 experiment (smx65 = 430.8W/m^2 and CO_2 = 460ppm) shows the fastest NH ice volume time-series increase at the start of the simulation, crossing the 15 msle threshold after only 18 kyrs of simulation. After that, the ice volume slightly decreases, stabilising at ~14.5 msle (Fig. 3). At the moment of crossing of the threshold, the ice sheet coverage over North America is larger than in the other two experiments, while no ice sheet develops over Scandinavia (Fig. 4c). For this case, the AMOC reaches equilibrium with a maximum strength of ~27 Sv in the second half of the simulation (Fig. 5). Deep convection is widespread in the North Atlantic, occurring over Labrador Sea, south of Greenland and Norwegian Sea (Fig. 6f). The Atlantic overturning circulation reaches depths of ~4000m (Fig. 6c).

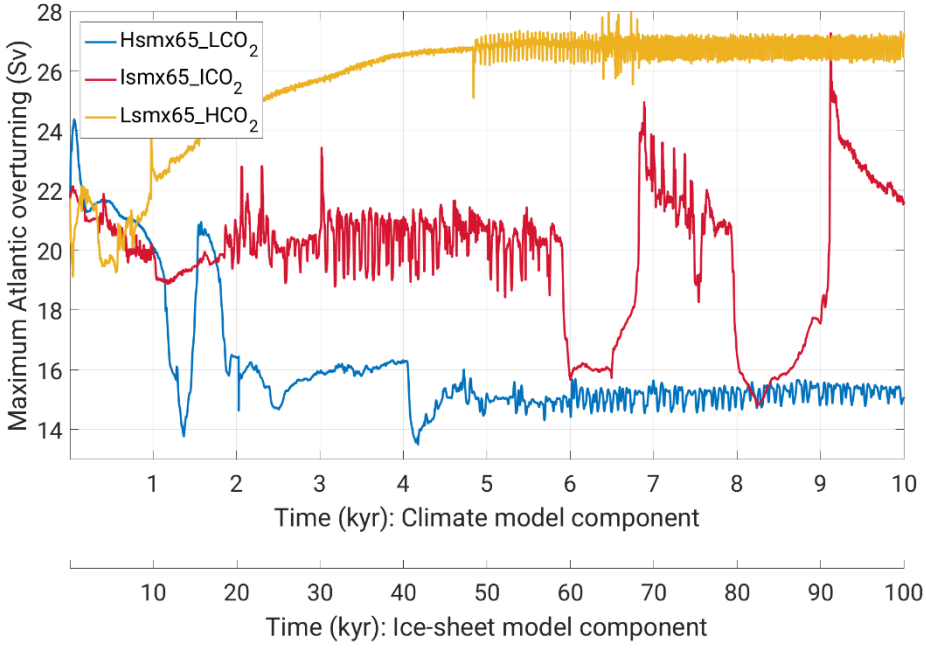

Figure 5: Maximum Atlantic Overturning (Sv) temporal evolution at the critical combination of smx65 and CO_2 for triggering glacial inception (threshold 15 msle level), for three selected experiments (see Table 1).

From these experiments it is clear that the timescales involved with glacial development in the vicinity of the glacial inception bifurcation point are extremely long and that even 100 kyrs of simulation might not be enough to reach stationary conditions. It is also clear that, in CLIMBER-X, glacial inception can occur for different AMOC configurations. The spatial patterns of glaciation are different and related to the AMOC intensity, with a weak AMOC transporting less heat from the tropics towards Scandinavia and facilitating ice growth there. We see that in CLIMBER-X, lower atmospheric CO_2 concentrations produce

https://doi.org/10.5194/cp-2023-81
Preprint. Discussion started: 4 October 2023
© Author(s) 2023. CC BY 4.0 License.

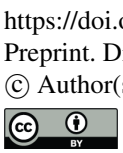

Climate of the Past Discussions
Open Access
EGU

weaker AMOC, a fact also observed in CLIMBER-2 (Bouttes et al., 2012; Gottschalk et al., 2019) and GCMs (e.g. Stouffer and Manabe, 2003; Galbraith and de Lavergne, 2019).

240

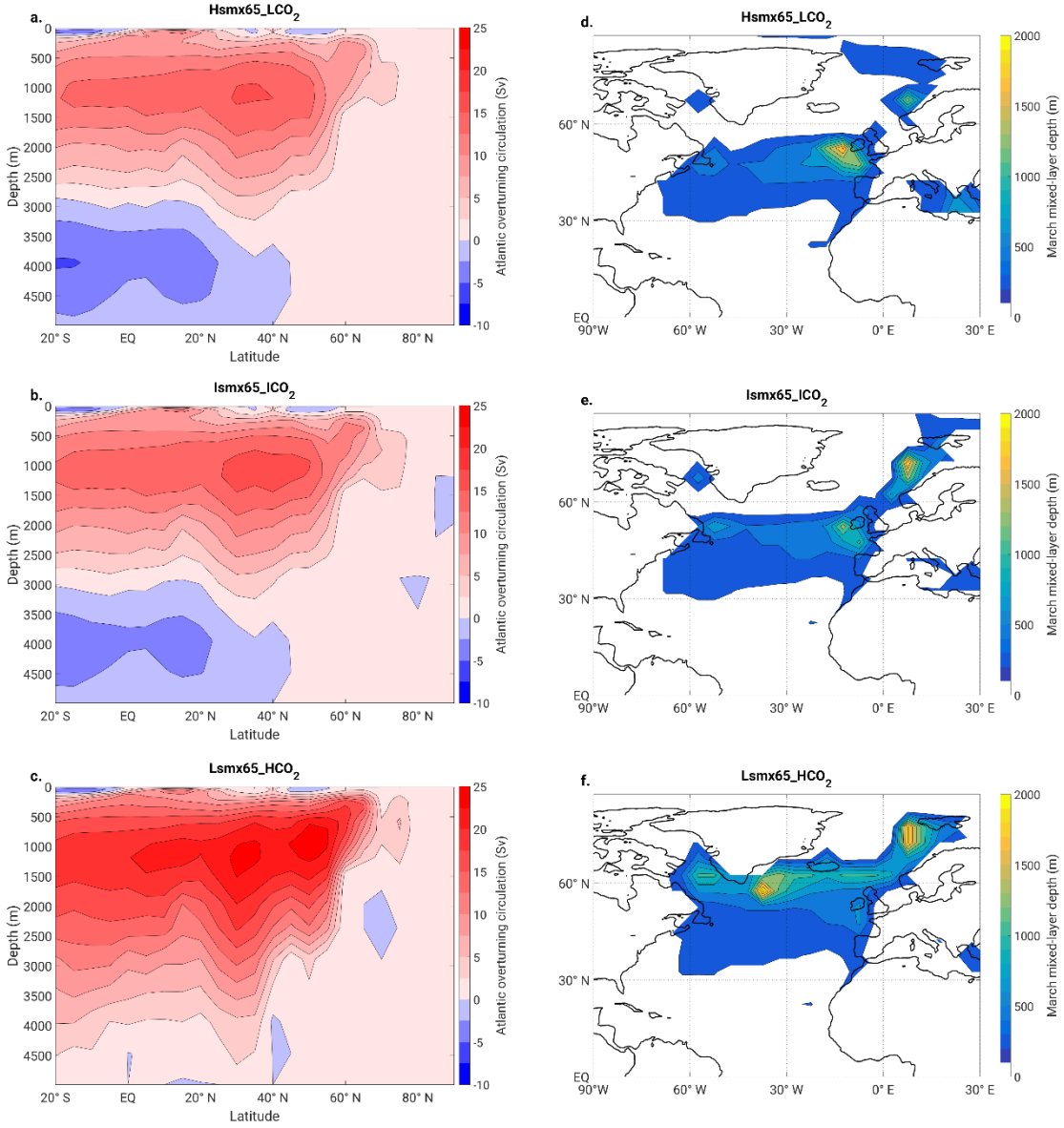

245 **Figure 6: Annual mean Atlantic Ocean meridional overturning circulation streamfunction (a-c) and maximum (March) mixed layer depth (d-f) for the experiments Hsmx65_LCO$_2$, Ismx65_ICO$_2$ and Lsmx65_HCO$_2$ at the time when each experiment reaches the 15 msle threshold.**

https://doi.org/10.5194/cp-2023-81
Preprint. Discussion started: 4 October 2023
© Author(s) 2023. CC BY 4.0 License.


To get a better understating on how different spatial patterns of ice growth arise with different combination of insolation and CO_2, we analyse the climatic conditions leading to the ice development. Figure 7 displays the annual-mean surface-mass balance (SMB) anomalies with respect to Control at the moment when the simulations reach the 15 msle of NH ice volume. For the three experiments, positive SMB anomalies with respect to Control are found over Greenland and over Baffin Island, the anomalies being larger in magnitude for the Lsmx65_HCO_2 case. For the Hsmx65_LCO_2 experiment, the largest positive anomalies occur over the Scandinavian Peninsula.

Given the fact that surface temperature and precipitation fields might be directly impacted by the presence of an ice sheet, we generate auxiliary experiments in which the conditions are the same as in Hsmx65_LCO_2, Ismx65_ICO_2 and Lsmx65_HCO_2 but without interactive ice sheets (i.e. the ice sheets remain constant and equal to the initial present-day conditions; Table 1) and denote them with an additional FixIce label.

Boreal summer (June-August; JJA) 2m temperature and annual precipitation anomalies with respect to Control in simulations without interactive ice sheets for the NH between 120°W and 60°E are displayed in Figure 8. For the Hsmx65_LCO_2_FixIce experiment, summer temperatures are lower are up to 6°C colder than in Control, with the coldest anomalies occurring over the North Atlantic Ocean. For the Ismx65_ICO_2_FixIce experiment, the 2m JJA temperatures are similar to Control_FixIce southward of 60°N and 1-2°C lower than Control_FixIce northward of 60°N. Last, in the Lsmx65_HCO_2_FixIce experiment, summer temperatures are warmer than in Control_FixIce over the Atlantic realm (with anomalies of up to 5°C) and similar to Control_FixIce over the continents. For the Hsmx_LCO_2_FixIce (Lsmx65_HCO_2_FixIce), the precipitation is lower (higher) than in Control_FixIce over the Atlantic basin north of 50°N, in the tropics a southward (northward) shift of the Intertropical Convergence Zone (ITCZ) is produced. Meanwhile, for Ismx65_ICO2, precipitation is similar to Control.

https://doi.org/10.5194/cp-2023-81
Preprint. Discussion started: 4 October 2023
© Author(s) 2023. CC BY 4.0 License.

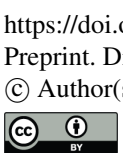

Climate of the Past Discussions
Open Access
EGU

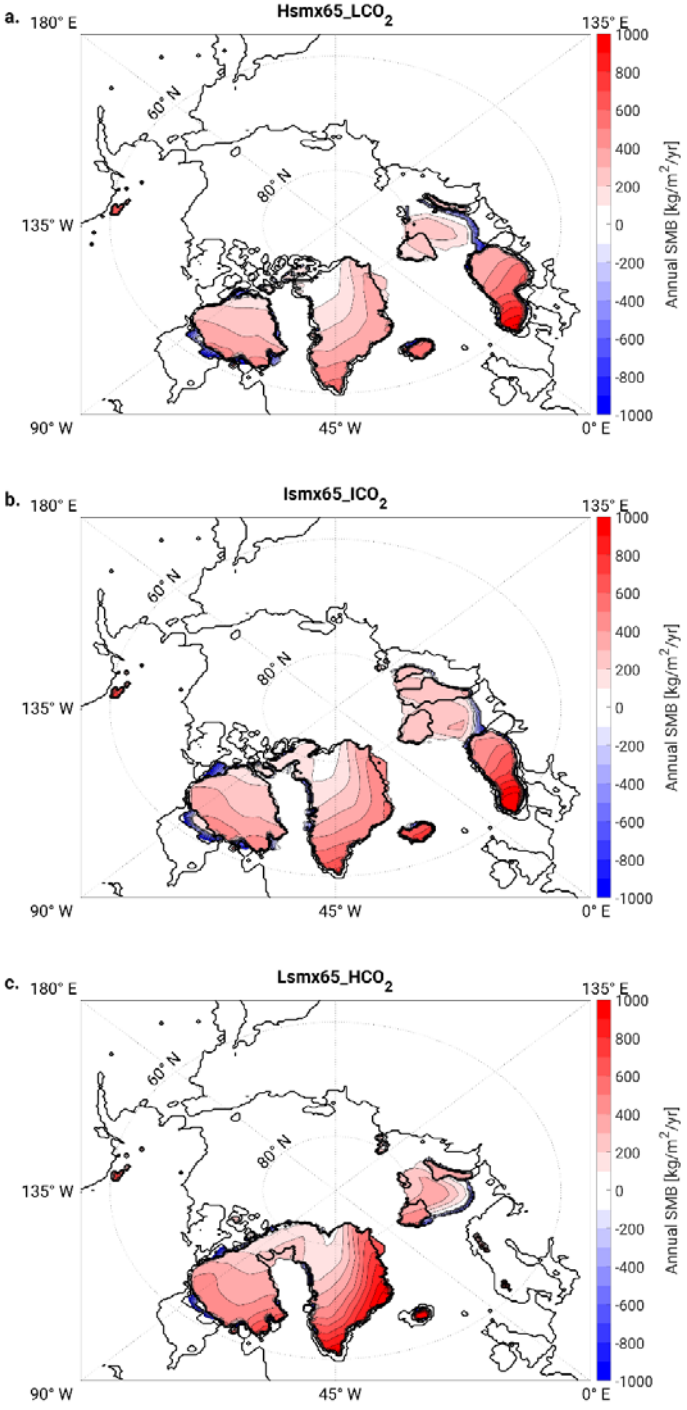

Figure 7: Annual surface mass balance anomaly with respect to Control for the experiments Hsmx65_LCO$_2$, Ismx65_ICO$_2$ and Lsmx65_HCO$_2$ (a-c), respectively, at the time when each experiment reaches the 15 msle threshold. Continental and ice sheet margins are show in black.

https://doi.org/10.5194/cp-2023-81
Preprint. Discussion started: 4 October 2023
© Author(s) 2023. CC BY 4.0 License.


This analysis highlights that, at the critical insolation-CO_2 limit, temperature and precipitation fields in areas where inception occurs can be different. For the case of high orbital forcing and low CO_2, colder than Control summer surface temperature is the main factor driving ice development. For the intermediate orbital forcing and intermediate CO_2, summer temperatures slightly colder than Control are enough to propitiate ice growth. However, for low orbital forcing and high CO_2, summer (and also winter; not shown) surface temperatures are, in most inception areas, higher than control and, therefore, do not explain the glacial inception. In that case, the climatic configuration that explains a positive SMB is annual precipitation, which is higher than Control in the areas where ice develops in the corresponding interactive ice-sheet simulations.

3.2 Role of AMOC change in glacial inception

To investigate the role of AMOC strength change at the glacial inception bifurcation limits, we produce a series of water hosing/extraction experiments (Table 1). The freshwater forcing is applied in the North Atlantic Ocean between 50°N and 70°N and compensated over the tropical (30°S-30°N) Pacific Ocean to prevent a global salinity drift. The magnitude of the freshwater flux is 0.01 Sv, either positive (added freshwater, leading to a weakening of AMOC) or negative (extracted freshwater, leading to a strengthening of AMOC). The hosing/extraction forcing is applied for the whole duration of the experiments. Note, that 0.01 Sv is a very small value compared to a typical stability threshold for AMOC in the CLIMBER-X model (Willeit et al., 2022).

The freshwater extraction produces less NH ice sheet volume in all three cases (Fig. 9). In particular, in the experiments Hsmx65_LCO$_2$ and Ismx65_ICO$_2$ the extraction in enough to prevent the NH ice volume to cross the 15 msle threshold used for the definition of glacial inception. In opposition, the freshwater hosing flux produces in all three cases a faster and larger ice growth in the NH. The largest change in terms if NH ice volume is produced for the Ismx65_ICO$_2$, reaching a magnitude of ~150 msle. In this case, the freshwater hosing flux produces the largest AMOC weakening of all three experiments, and even an almost complete AMOC shutdown between 50 and 80 kyrs of the simulation (Fig. 10).

This set of hosing experiments shows that AMOC (in particular its stability) plays a role in the triggering of glacial inception and the rate of ice growth. In general, the weaker the AMOC the larger and faster the development of the NH ice sheets, for a given insolation/CO_2 pairing.

https://doi.org/10.5194/cp-2023-81
Preprint. Discussion started: 4 October 2023
© Author(s) 2023. CC BY 4.0 License.

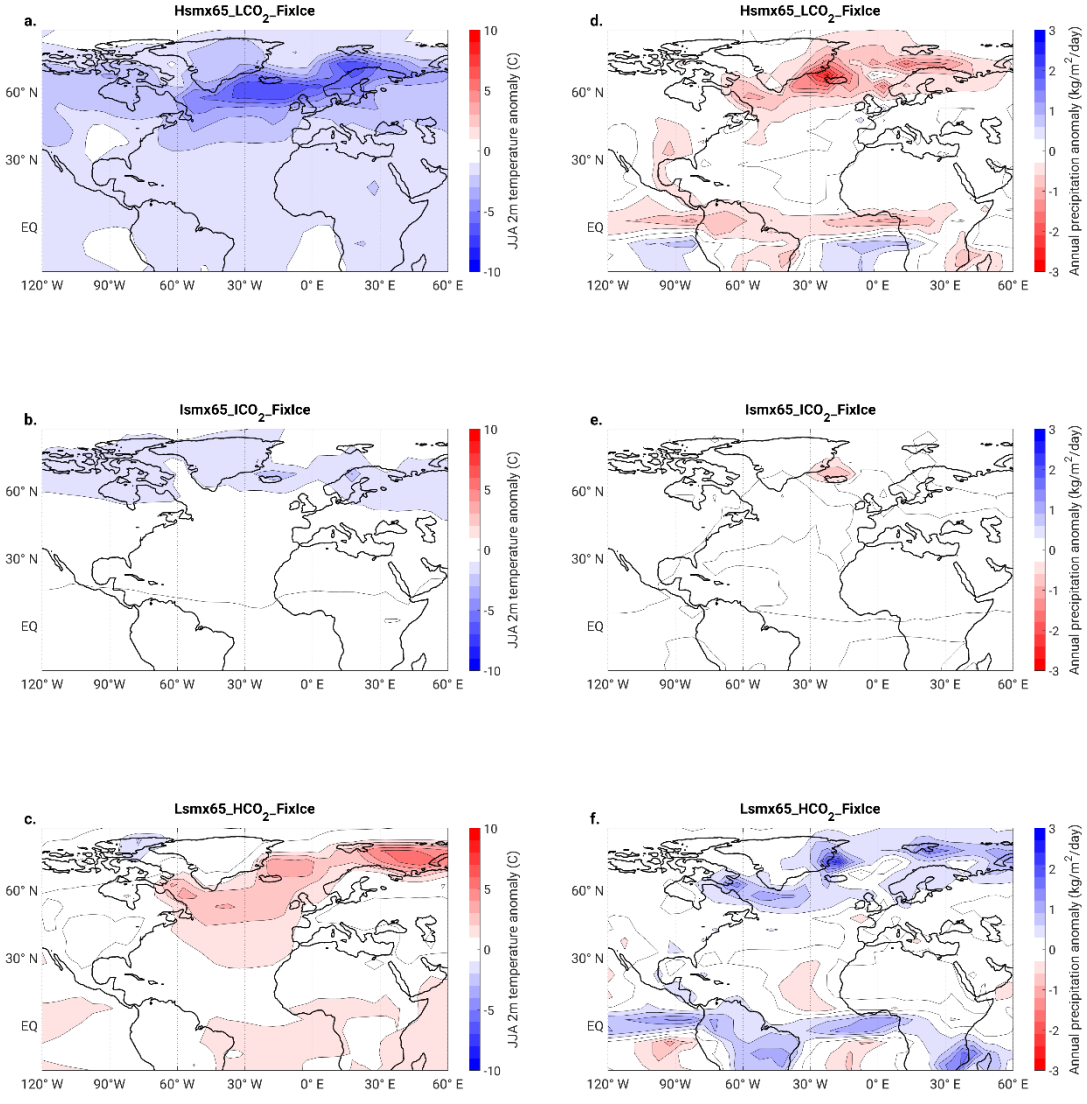

Figure 8: a, b, c Summer (JJA) and d, e, f annual precipitation anomalies with respect to Control_FixIce for experiments Hsmx65_LCO2_FixIce, Ismx65_ICO2_FixIce and Lsmx65_CO2_FixIce. Control continental margins (present-day conditions) are shown in black.

https://doi.org/10.5194/cp-2023-81
Preprint. Discussion started: 4 October 2023
© Author(s) 2023. CC BY 4.0 License.

Climate of the Past Discussions
Open Access
EGU

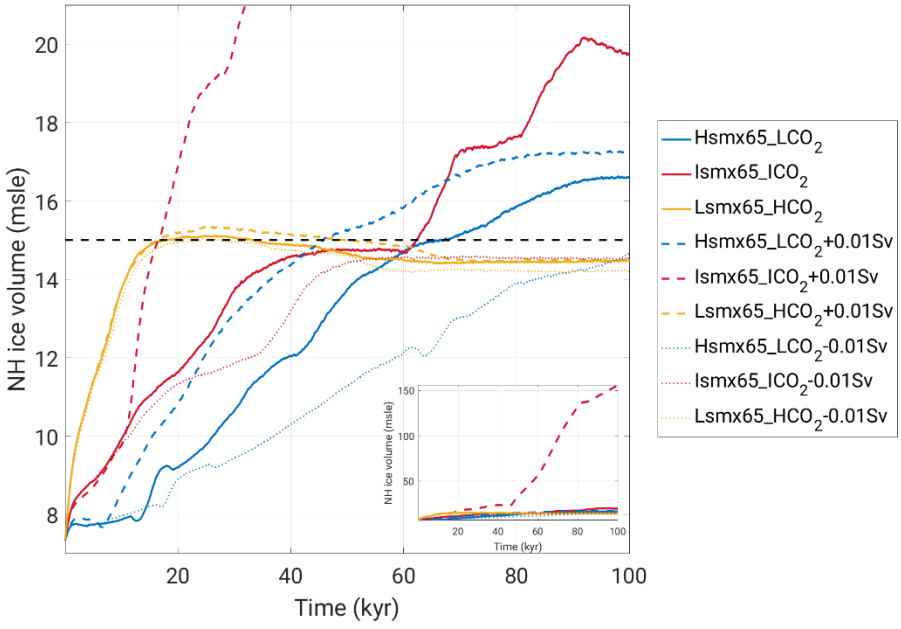

Figure 9: NH ice volume (msle) temporal evolution in water hosing/extraction experiments (Table 1).

330

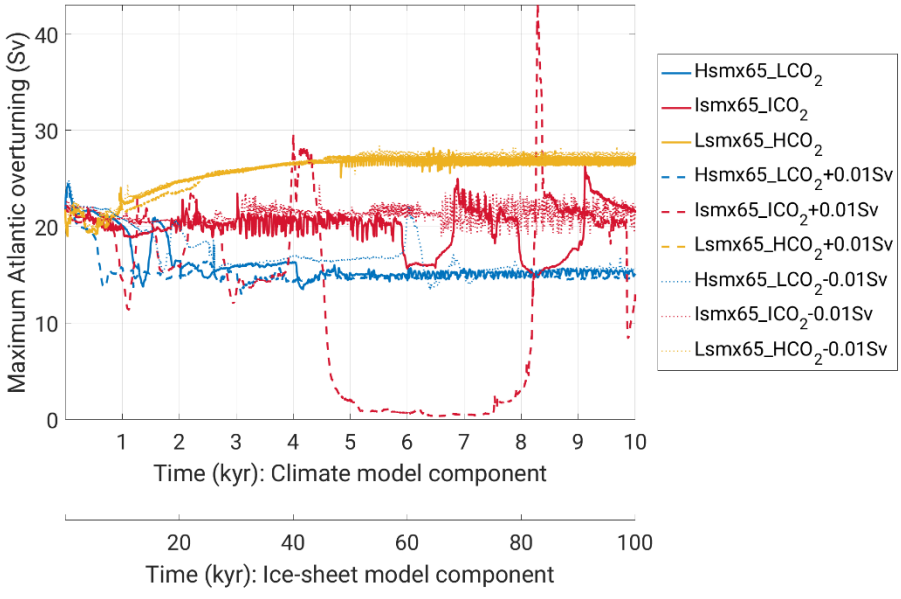

Figure 10: Maximum Atlantic overturning (Sv) temporal evolution in water hosing/extraction experiments (Table 1).

https://doi.org/10.5194/cp-2023-81
Preprint. Discussion started: 4 October 2023
© Author(s) 2023. CC BY 4.0 License.

Climate of the Past Discussions

3.3 Suitability of smx65 as proxy for orbital forcing

The usage of smx65 as a proxy for orbital forcing in the tracing of the glacial inception bifurcation is justified by the relevance of the 65°N latitude for the development of ice sheets (Ganopolski, 2023). However, as seen in Fig. 2 this metric is not perfect: for example, in two experiments with very similar value of smx65 (~462 W/m^2), the CO_2 critical for triggering glacial inception differs by 25 ppm. This discrepancy highlights that, although useful, smx65 is perhaps not always the most adequate metric for evaluating glacial inception.

To evaluate the possibility of using other proxies, we start by separating the smx65 time-series into its obliquity and precessional components (as in Jackson and Broccoli, 2003). The decomposition is done via a least-squares fit to the data of the last 400 kyr, expressing the smx65 time-series in the form:

$$smx65 = a_0 + a_1 * ecc * \sin\omega + a_2 * (obl - \overline{obl}) \quad (2)$$

With ecc, ω and obl denoting eccentricity, longitude of perihelion and obliquity, respectively; coefficients a_0, a_1, and a_2 are derived from the least-squares fit and the over bar indicates time averaging. The precessional (smx_p) and obliquity (smx_o) components are defined as:

$$smx65\_p = a_0 + a_1 * ecc * \sin\omega \quad (3)$$

$$smx65\_o = a_2 * (obl - \overline{obl}) \quad (4)$$

We systematically analyse the use of linear combinations of smx65_p and smx65_o as alternative proxies for orbital forcing. We wish to find γ, which maximises the goodness-of-fit (R^2- coefficient of determination) between the logarithm of critical CO_2 and the proposed proxy: $smx65_p + \gamma * smx65\_o$.

Any value of γ between 1 and 2 yields an extremely good fit (R^2 higher than 0.95) and, thus, the quantities $smx65_p + \gamma * smx65\_o$ for those values of γ are good proxies for orbital forcing (Fig. 11). Values of γ lower than 1, in which the contribution of obliquity is considered relatively less important than that of precession, are not optimal proxies. Similarly, values of γ higher than 2 (i.e. the obliquity contribution is weighted more than the precessional one) are also not adequate. Therefore, γ=1, which corresponds to using the smx65 time-series as proxy metric of orbital forcing, is indeed adequate and close to being the best possibility among the tested options.

https://doi.org/10.5194/cp-2023-81
Preprint. Discussion started: 4 October 2023
© Author(s) 2023. CC BY 4.0 License.

Climate of the Past Discussions

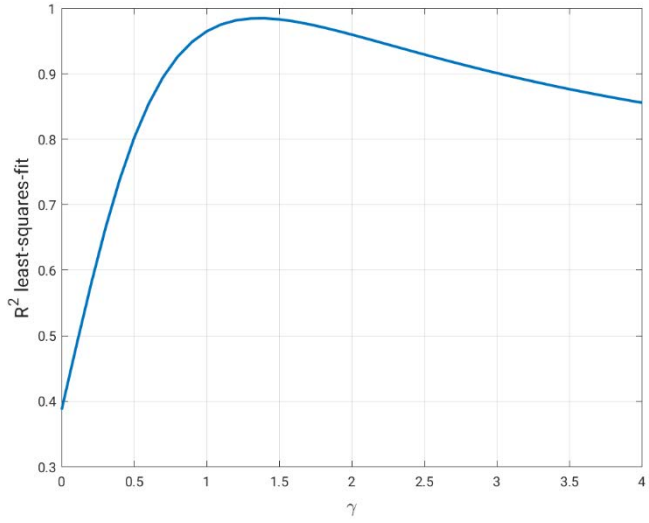

Figure 11: Goodness-of-fit (R^2 coefficient of determination) derived from the least-squares-fit between $\ln(CO_{2\ critical})$ and smx65_p + γ*smx65_o as a function of γ, considering CO_2 values critical for glacial inception at the 15 msle level.

4 Summary and conclusions

We used the recently developed EMIC CLIMBER-X to produce a new estimation of the critical insolation – CO_2 relationship for triggering glacial inception. The use of CLIMBER-X for tracing the glacial inception bifurcation constitutes a further development from previous attempts produced with the coarser-resolution and simpler CLIMBER-2 model (Ganopolski et al., 2016; Archer and Ganopolski, 2005).

The study is based on sets of equilibrium experiments in which the orbital parameters and atmospheric CO_2 concentration are kept constant in time. The sets are based on orbital configurations corresponding to all the local minima of summer maximum insolation at 65°N (smx65) of the last 400 kyr. Therefore, our experiments reflect a diverse arrangement of orbital parameters in configurations potentially favourable for glacial inception. The estimation of the glacial inception bifurcation is done within a 5 ppm resolution in the CO_2 phase-space.

The new estimation of the critical insolation – CO_2 relationship for triggering glacial inception follows a logarithmic dependence, explained by the logarithmic shape of the radiative forcing of CO_2. When considering that glacial inception occurs if the NH ice volume develops at least 15 msle, the new CLIMBER-X estimation for the critical summer maximum insolation at 65°N and CO_2 relationship is:

https://doi.org/10.5194/cp-2023-81
Preprint. Discussion started: 4 October 2023
© Author(s) 2023. CC BY 4.0 License.

Climate of the Past Discussions

$$smx65_{cr}[W/m^2] = -75 * \ln\left(\frac{CO_2\ [ppm]}{280}\right) + 465 \quad (5)$$

This new estimation is close to the one produced with CLIMBER-2 in Ganopolski et al. (2016), who used a similar threshold for NH ice volume. Moreover, we showed that the summer maximum insolation at 65°N is a skilful single metric for tracing the glacial inception bifurcation.

We also showed that the temporal and spatial patterns of glacial inception are not always the same, but depend on the combination of insolation and critical CO_2 concentration. The time needed for reaching the glacial inception bifurcation threshold varies between 18 and almost 100 thousand years, highlighting the long timescales involved at the bifurcation limit. The spatial patterns of ice sheets growth during glacial inception depict ice development outside of Greenland north of Hudson Bay in North America, Iceland and Svalbard. Considerable ice growth over the Scandinavian Peninsula is only observed in experiments in which the Atlantic Meridional Overturning Circulation (AMOC) significantly weakens, which occurs in either low CO_2 cases (stable weak AMOC) or intermediate CO_2 situations (unstable AMOC with substantial weakening episodes). In general, the lower the CO_2, the weaker the AMOC and, thus, the weaker the heat transport from the tropics towards European high latitudes, facilitating the Scandinavian ice sheet development.

5 Annex A: Theoretical derivation of the critical insolation-CO_2 relationship

To derive the critical insolation-CO_2 relationship for triggering glacial inception, we consider the surface energy balance of snow cover at the location where the nucleation of the northern continental ice sheet begins during glacial inceptions. Important assumptions are:

(i) this location remains the same for the different combinations of insolation and CO_2

(ii) glacial inception begins from the formation of extensive perennial snowfields rather than from the spreading of glaciers from high mountains.

Both these assumptions are consistent with the results of our model simulations.

Surface daily mass balance of the snowpack during the melt season is described by the following equation:

$$S_{abs} + R_{\downarrow} - R_{\uparrow} + H = ML \quad (A1)$$

where S_{abs} is the absorbed short-wave radiation, $R_{\downarrow}$ is the downward long-wave radiation flux near the earth surface, $R_{\uparrow}$ is the longwave radiation emitted by the snow surface, H is the sensible heat flux (positive downward), M is the snow melt rate in kg m^{-2} s^{-1}, and L is the latent heat of fusion. Surface latent heat flux can be neglected during the melt season. Since we consider only the period of snow-melt, surface temperature during this period is 0ºC. In this case, the terms in the left-hand side of the eq. (A1) can be expressed as follows:

https://doi.org/10.5194/cp-2023-81
Preprint. Discussion started: 4 October 2023
© Author(s) 2023. CC BY 4.0 License.

Climate of the Past Discussions

$$S_{abs} = S(1-\alpha_S)\tau \quad \text{(A2)}$$

$$R_{\downarrow} = F(0) + \beta T \quad \text{(A3)}$$

$$R_{\uparrow} = \varepsilon\,\sigma\,T_0^4 \quad \text{(A4)}$$

$$H = \gamma\,T \quad \text{(A5)}$$

where T is the surface air temperature (in °C), S is the insolation at the top of the atmosphere, α_s is the surface albedo, τ is the atmospheric transmissivity, $F(0)$ is the downward long-wave radiation for a surface air temperature of 0°C in W/m^2, T_0=273.15 K, σ=5.67 10^{-8} W m^{-2} K^{-4} is the Stefan-Boltzmann constant, $\varepsilon \approx 1$ is the snow emissivity for long-wave radiation, β and γ are empirical parameters.

In the nucleation centre of glacial inception (northern Canada and Baffin Island), the melt-season is only about two months and approximately coincides with the period of positive air temperatures. This allows us to make further simplifications when integrating eq. (A1) over the melt season after substituting eq. (A2-5):

$$\bar{S}(1-\alpha_S)\tau + F(0) + \beta\bar{T} - \sigma T_0^4 + \gamma\bar{T} = \bar{M}\,L \quad \text{(A6)}$$

where $\bar{T}$ is the surface air temperature, $\bar{S}$ is daily insolation and $\bar{M}$ is snowmelt, all averaged over the melt season. Assuming that the duration of the melt season at the location of glacial inception is about two months (which is similar to present climate conditions in the area where glacial inception is simulated in CLIMBER-X), the seasonal surface air temperature evolution can be approximated by a sinusoidal function with zero air temperatures at the beginning and end of the melt season and the average insolation and temperature can be expressed through their maximum annual values as

$$\bar{S} = k_S\,smx65 \quad , \quad \bar{T} = k_T\,T_{max},$$

where $k_S \approx 0.9$ and $k_T \approx 0.7$. Maximum summer air temperature is parameterized as

$$T_{max} = T^*_{max} + \delta \ln\left(\frac{CO_2}{CO_{2_0}}\right) + \mu\,(smx65 - smx65^*) \quad \text{(A7)}$$

where T^*_{max} is the maximum summer temperature at the location of glacial inception for preindustrial conditions, namely for $C0_2$=CO_{2_0} and $smx65$=$smx65^*$, where CO_2 is atmospheric CO_2 concentration, $C0_{2\_0}$ = 280 ppm, and smx65*= 479 W/m^2 is the present-day maximum insolation at 65°N. The parameter μ represents the sensitivity of summer temperature at the location of glacial inception to summer insolation, i.e.

$$\mu = \frac{\Delta T_{max}}{\Delta smx65}$$

The parameter δ in eq. (A7) represents the sensitivity of maximum summer temperature to CO_2 concentration. It can be expressed through other known parameters as $\delta = p_a\,r_f\,c_s$, where p_a is the "polar amplification" of maximum summer temperature equal to $\Delta T_{max}/\Delta T_g$, where ΔT_g is the global air temperature anomaly caused by CO_2 concentration change, r_f is the parameter determining radiative forcing of CO_2:

$$\Delta R_{CO_2} = r_f \ln\left(\frac{CO_2}{CO_{2\_0}}\right)$$

https://doi.org/10.5194/cp-2023-81
Preprint. Discussion started: 4 October 2023
© Author(s) 2023. CC BY 4.0 License.

Climate of the Past Discussions

and c_s is the specific climate sensitivity (e.g. Rohling et al., 2012) which relates the global temperature change to radiative forcing:

$$\Delta T_g = c_S \, \Delta R$$

Based on IPCC (2021) and climate model simulations p_a=1.5, r_f =5.7 W m^{-2}, and c_s=0.75 ^{o}C W^{-1} m^2, which is equivalent to an equilibrium climate sensitivity of 3^{o}C. Thus δ=6.4^{o}C.

To derive a critical relationship between insolation and CO_2 for triggering glacial inception, we make use of the fact that the glacial inception occurs when the total snowmelt minus refreezing during the melt season does not exceed annual snowfall P (in kg m^{-2}), which for the considered region is less than 200 kg m^{-2} :

$$\bar{M}\Delta t_M = \frac{P}{(1-f_r)}$$

where Δt_M is the duration of the melt season and f_r is an average refreezing fraction of snowmelt. Thus, eq. (A6) can be re-written as:

$$k_S(1-\alpha_S)\tau \, smx65 + k_T(\beta+\gamma)\left(\delta \ln\left(\frac{CO_2}{CO_{2_0}}\right) + \mu \, smx65\right) = \frac{PL}{(1-f_r)\Delta t_M} + \sigma T_0^4 - F(0) - k_T(\beta+\gamma)(T^*_{max} - \mu \, smx65^*) \quad \text{(A8)}$$

which can be rewritten in the form:

$$smx65cr = A - B \ln\left(\frac{CO_2}{CO_{2\_0}}\right) \quad \text{(A9)}$$

which is identical to the relationship proposed in Ganopolski et al. (2016). Here

$$A = \frac{PL(1-f_r)^{-1}\Delta t_M^{-1} + \sigma T_0^4 - F(0) + k_T(\beta+\gamma)(\mu smx65^* - T^*_{max})}{k_S(1-\alpha_S)\tau + k_T\mu(\beta+\gamma)} \quad \text{(A10)}$$

and

$$B = \frac{k_T\delta(\beta+\gamma)}{k_S(1-\alpha_S)\tau + k_T\mu(\beta+\gamma)} \quad \text{(A11)}$$

We will start from determining B, which can be calculated using the following values of model parameters: α_s=0.7, which is a typical albedo of melting snow, τ=0.5 is taken from Robinson et al. (2010), β=4 W m^{-2} ^{o}C^{-1} (derived from the regression of model data for the considered region), γ=15 W m^{-2} ^{o}C^{-1} (middle of the range from Braithwaite, 2009), μ=0.08 W^{-1} m^2 ^{o}C (from climate model simulations for different orbital parameters). However, since $k_S(1-\alpha_S)\tau = 0.13 \ll k_T(\beta+\gamma) = 0.9$, eq. (A11) for B can be significantly simplified, and only two parameters are required:

$$B = \frac{\delta}{\mu} \approx 80 \, W/m^2 \quad \text{(A12)}$$

Equation (A10) for A contains a number of parameters which are not accurately known. However, knowledge of all these parameters is not required. It is only essential that the value of A for different glacial inceptions should remain approximately constant. This requirement is satisfied since only the total snowfall depends on the values of insolation and CO_2 in this formula. However, the contribution of the latent heat term $PL(1-f_r)\Delta t_M$ to the value of A is only about 10-20%, and, according to

https://doi.org/10.5194/cp-2023-81
Preprint. Discussion started: 4 October 2023
© Author(s) 2023. CC BY 4.0 License.

Climate of the Past Discussions

climate model simulations, changes in annual precipitation for a wide range of CO_2 concentrations are of the same magnitude. Thus, the total variations of A across the considered range of climate conditions should not exceed few percents. This allows us to determine A using two paleoclimate constraints, namely, that glacial inceptions occurred at the end of MIS 19 and 11, while no glacial inception occurred in the recent past (see also Fig. 3b in Ganopolski et al., 2016). These empirical constraints suggest that under the present-day maximum summer insolation of 479 W/m^2, glacial inception can only occur if CO_2 concentration is around 240 ppm. This gives the following value:

$$A = 479 + 80\ln\left(\frac{240}{280}\right) \approx 467 \text{ W/m}^2$$

Note that the choice of critical CO_2 for present day insolation of 240±20ppm, results in the uncertainty of A only ±6 W/m^2. Equation (A9) now can be rewritten as:

$$smx65_{cr}[W/m^2] = -80 * \ln\left(\frac{CO_2\ [ppm]}{280}\right) + 467$$

which is numerically very similar to Ganopolski et al. (2016) and the results of the present study.

Equation (A12) for B has a clear physical sense: the slope of the critical relationship between insolation and the logarithm of CO_2 concentration is equal to the ratio between local temperature sensitivities to CO_2 (δ) and summer insolation (μ). This value has dimension W/m^2. If one wants to compare the effect of insolation to the effect of radiative forcing of CO_2 in the same units of W/m^2, then it would be B/r_f =15, i.e. one W/m^2 of CO_2 forcing is approximately equivalent to 15 W/m^2 of the maximum summer insolation in determining the glacial inception. This number is consistent with the results of earlier studies (Calov and Ganopolski, 2005; Abe-Ouchi et al., 2013).

Code and data availability

Code and data used in this study can be obtained from https://doi.org/10.17605/OSF.IO/2MHKY (Talento, 2023).

Author contribution

ST performed all simulations and figures. All authors contributed to the analysis of results and preparation of the manuscript.

Competing interests

The authors declare that they have no conflict of interest.

Financial support

Financial support for ST was provided by the Swiss National Cooperative for the Disposal of Radioactive Waste (NAGRA).

https://doi.org/10.5194/cp-2023-81
Preprint. Discussion started: 4 October 2023
© Author(s) 2023. CC BY 4.0 License.

6 References

505 Abe-Ouchi, A., Saito, F., Kawamura, K., Raymo, M. E., Okuno, J. I., Takahashi, K., & Blatter, H. (2013). Insolation-driven 100,000-year glacial cycles and hysteresis of ice-sheet volume. *Nature*, *500*(7461), 190-193. https://doi.org/10.1038/nature12374

Archer, D., & Ganopolski, A. (2005). A movable trigger: Fossil fuel CO2 and the onset of the next glaciation. *Geochemistry, Geophysics, Geosystems*, *6*(5). https://doi.org/10.1029/2004GC000891

510 Bouttes, N., Roche, D. M., & Paillard, D. (2012). Systematic study of the impact of fresh water fluxes on the glacial carbon cycle. *Climate of the Past*, *8*(2), 589-607. https://doi.org/10.5194/cp-8-589-2012

515 Braithwaite, R.J., (2009) Calculation of sensible-heat flux over a melting ice surface using simple climate data and daily measurements of ablation. Annals of Glaciology, 50, 9-15. https://doi.org/10.3189/172756409787769726

Calov, R., Ganopolski, A., Claussen, M., Petoukhov, V., & Greve, R. (2005). Transient simulation of the last glacial inception. Part I: glacial inception as a bifurcation in the climate system. *Climate Dynamics*, *24*, 545-561. https://doi.org/10.1007/s00382-
520 005-0007-6

Calov, R., and A. Ganopolski (2005) Multistability and hysteresis in the climate-cryosphere system under orbital forcing, Geophys. Res. Lett., 32, L21717. https://doi.org/10.1029/2005GL024518

525 Galbraith, E., & de Lavergne, C. (2019). Response of a comprehensive climate model to a broad range of external forcings: relevance for deep ocean ventilation and the development of late Cenozoic ice ages. *Climate Dynamics*, *52*, 653-679. https://doi.org/10.1007/s00382-018-4157-8

Ganopolski, A. (2023). Toward Generalized Milankovitch Theory (GMT). *Climate of the Past Discussions*, *2023*, 1-71.
530 https://doi.org/10.5194/cp-2023-57

Ganopolski, A., Petoukhov, V., Rahmstorf, S., Brovkin, V., Claussen, M., Eliseev, A., & Kubatzki, C. (2001). CLIMBER-2: a climate system model of intermediate complexity. Part II: model sensitivity. *Climate Dynamics*, *17*, 735-751. https://doi.org/10.1007/s003820000144

535

© Author(s) 2023. CC BY 4.0 License.

Ganopolski, A., & Brovkin, V. (2017). Simulation of climate, ice sheets and CO 2 evolution during the last four glacial cycles with an Earth system model of intermediate complexity. *Climate of the Past*, *13*(12), 1695-1716. https://doi.org/10.5194/cp-13-1695-2017

Ganopolski, A., Calov, R., & Claussen, M. (2010). Simulation of the last glacial cycle with a coupled climate ice-sheet model of intermediate complexity. *Climate of the Past*, *6*(2), 229-244. https://doi.org/10.5194/cp-6-229-2010

Ganopolski, A., Winkelmann, R., & Schellnhuber, H. J. (2016). Critical insolation–CO2 relation for diagnosing past and future glacial inception. *Nature*, *529*(7585), 200-203. https://doi.org/10.1038/nature16494

Greve, R., Calov, R., & Herzfeld, U. C. (2017). Projecting the response of the Greenland ice sheet to future climate change with the ice sheet model SICOPOLIS. *低温科学*, *75*, 117-129. https://doi.org/10.14943/lowtemsci.75.117, 2017

Gottschalk, J., Battaglia, G., Fischer, H., Frölicher, T. L., Jaccard, S. L., Jeltsch-Thömmes, A., ... & Stocker, T. F. (2019). Mechanisms of millennial-scale atmospheric CO2 change in numerical model simulations. *Quaternary science reviews*, *220*, 30-74. https://doi.org/10.1016/j.quascirev.2019.05.013

IPCC, 2021: Climate Change 2021: The Physical Science Basis. Contribution of Working Group I to the Sixth Assessment Report of the Intergovernmental Panel on Climate Change [Masson-Delmotte, V., P. Zhai, A. Pirani, S.L. Connors, C. Péan, S. Berger, N. Caud, Y. Chen, L. Goldfarb, M.I. Gomis, M. Huang, K. Leitzell, E. Lonnoy, J.B.R. Matthews, T.K. Maycock, T. Waterfield, O. Yelekçi, R. Yu, and B. Zhou (eds.)]. Cambridge University Press, Cambridge, United Kingdom and New York, NY, USA.

Jackson, C. S., & Broccoli, A. J. (2003). Orbital forcing of Arctic climate: mechanisms of climate response and implications for continental glaciation. *Climate Dynamics*, *21*, 539-557. https://doi.org/10.1007/s00382-003-0351-3

Köhler, P., Bintanja, R., Fischer, H., Joos, F., Knutti, R., Lohmann, G., & Masson-Delmotte, V. (2010). What caused Earth's temperature variations during the last 800,000 years? Data-based evidence on radiative forcing and constraints on climate sensitivity. *Quaternary Science Reviews*, *29*(1-2), 129-145. https://doi.org/10.1016/j.quascirev.2009.09.026

Klemann, V., Martinec, Z., & Ivins, E. R. (2008). Glacial isostasy and plate motion. *Journal of Geodynamics*, *46*(3-5), 95-103. https://doi.org/10.1016/j.jog.2008.04.005, 2008

© Author(s) 2023. CC BY 4.0 License.

Laskar, J., Robutel, P., Joutel, F., Gastineau, M., Correia, A. C., & Levrard, B. (2004). A long-term numerical solution for the insolation quantities of the Earth. *Astronomy & Astrophysics*, *428*(1), 261-285. https://doi.org/10.1051/0004-6361:20041335

Leloup, G., & Paillard, D. (2022). Influence of the choice of insolation forcing on the results of a conceptual glacial cycle model. *Climate of the Past*, *18*(3), 547-558. https://doi.org/10.5194/cp-18-547-2022

Martinec, Z., Klemann, V., van der Wal, W., Riva, R. E. M., Spada, G., Sun, Y., ... & James, T. S. (2018). A benchmark study of numerical implementations of the sea level equation in GIA modelling. *Geophysical Journal International*, *215*(1), 389-414. https://doi.org/10.1093/gji/ggy280

Milankovitch, M. M. (1941). Canon of insolation and the iceage problem. *Koniglich Serbische Akademice Beograd Special Publication*, *132*.

Paillard, D. (1998). The timing of Pleistocene glaciations from a simple multiple-state climate model. *Nature*, *391*(6665), 378-381. https://doi.org/10.1038/34891

Petoukhov, V., Ganopolski, A., Brovkin, V., Claussen, M., Eliseev, A., Kubatzki, C., & Rahmstorf, S. (2000). CLIMBER-2: a climate system model of intermediate complexity. Part I: model description and performance for present climate. *Climate dynamics*, *16*, 1-17. https://doi.org/10.1007/PL00007919

Robinson, A., Calov, R., & Ganopolski, A. (2010). An efficient regional energy-moisture balance model for simulation of the Greenland Ice Sheet response to climate change. *The Cryosphere*, *4*(2), 129-144. https://doi.org/10.5194/tc-4-129-2010, 2010

Rohling, E. J., Sluijs, A., Dijkstra, H. A., Köhler, P., van de Wal, R.,S. W., von der Heydt, A. S., Beerling, D. J., Berger, A., Bijl, P. K., Crucifix, M., DeConto, R., Drijfhout, S. S., Fedorov, A., Foster, G. L., Ganopolski, A., Hansen, J., Hönisch, B., Hooghiemstra, H., Huber, M., Huybers, P., Knutti, R., Lea, D. W., Lourens, L. J., Lunt, D., Masson-Demotte, V., Medina-Elizalde, M., Otto-Bliesner, B., Pagan, M., Pälike, H., Renssen, H., Royer, D. L., Siddall, M., Valdes, P., Zachos, J. C., and Zeebe, R. E. (2012) Making sense of palaeoclimate sensitivity. Nature, 491, 683–691. https://doi.org/10.1038/nature11574

Stouffer, R. J. & Manabe, S. Equilibrium response of thermohaline circulation to large changes in atmospheric CO2 concentration. *Clim. Dyn.* **20**, 759–773 (2003).

Talento, S. (2023). Code and data: New estimation of critical insolation – CO_2 relationship for triggering glacial inception. OSFHome [data set and code], https://doi.org/10.17605/OSF.IO/2MHKY

© Author(s) 2023. CC BY 4.0 License.

Talento, S., & Ganopolski, A. (2021). Reduced-complexity model for the impact of anthropogenic CO 2 emissions on future glacial cycles. *Earth System Dynamics*, *12*(4), 1275-1293. https://doi.org/10.5194/esd-12-1275-2021

Willeit, M., Ganopolski, A., Calov, R., & Brovkin, V. (2019). Mid-Pleistocene transition in glacial cycles explained by declining CO2 and regolith removal. *Science Advances*, *5*(4), eaav7337. https://doi.org/10.1126/sciadv.aav7337

Willeit, M., Ganopolski, A., Robinson, A., & Edwards, N. R. (2022). The Earth system model CLIMBER-X v1. 0–Part 1: Climate model description and validation. *Geoscientific Model Development*, *15*(14), 5905-5948. https://doi.org/10.5194/gmd-15-5905-2022

Willeit, M., Ilyina, T., Liu, B., Heinze, C., Perrette, M., Heinemann, M., ... & Ganopolski, A. (2023a). The earth system model CLIMBER-X v1. 0-Part 2: The global carbon cycle. *Geophysical Model Development*, *16*, 3501-3534. https://doi.org/10.5194/gmd-2022-307

Willeit, M., Calov, R., Talento, S., Greve, R., Bernales, J., Klemann, V., Bagge, M., and Ganopolski, A. (2023b): Glacial inception through rapid ice area increase driven by albedo and vegetation feedbacks, EGUsphere [preprint], https://doi.org/10.5194/egusphere-2023-1462